Hindawi
Indoor Air
Volume 2023, Article ID 7940661, 19 pages
https://doi.org/10.1155/2023/7940661

Research Article

The Inherent Instability of Environmental Parameters Governing Indoor Air Quality on Board Ships and the Use of Temporal Trends to Identify Pollution Sources

Olivier Schalm,[1] **Gustavo Carro**,[1,2] **Werner Jacobs**,[1] **Borislav Lazarov**,[3] **and Marianne Stranger**[3]

[1]*Antwerp Maritime Academy, Belgium*
[2]*Department of Mathematics, Computer Science, University of Antwerp, Belgium*
[3]*Flemish Institute for Technological Research (VITO), Mol, Belgium*

Correspondence should be addressed to Olivier Schalm; olivier.schalm@hzs.be

Received 21 November 2022; Revised 11 March 2023; Accepted 23 March 2023; Published 22 April 2023

Academic Editor: Rahil Changotra

Indoor air quality on board a 36-year-old ship has been characterized at several locations. The ship is dedicated to nearshore operations at the Belgian coast. This paper presents time-averaged and continuous-time measurements of several indoor pollutant concentrations such as NO_2, O_3, NO, CO, total volatile organic compounds (TVOC), polycyclic aromatic hydrocarbons (PAH), particulate matter $PM_{2.5}$ and PM_{10}, black carbon, and individual organic compounds. Time-averaged measurements suggest that the ship's indoor air quality is sufficiently safe according to the prescribed occupational and nonoccupational health limits. However, the concentration of some indoor pollutants is comparable to that of the outdoor air of a large city such as Brussels, Belgium. Continuous-time analyses show that the temporal trends of indoor pollutant concentrations are inherently unstable. A large number of peaks or valleys are observed on a slowly fluctuating background. At some occasions, pollutant concentrations exceed the nonoccupational thresholds. Several pollutant peaks occur simultaneously, resulting in a pattern of peaks that is typical for a pollution source (e.g., exhaust gases entering the ship's castle through the ventilation inlet, human presence, and bunkering). This study illustrates that multiparameter monitoring campaigns give valuable information about the behaviour of pollution sources, facilitating the definition of mitigation actions.

1. Introduction

Ship exhaust emissions are analysed for several reasons such as estimating the emission contribution of ships to local air quality [1–4], understanding the relation between pollution and shipping lanes [5], or the long-term emission prognosis according to several scenarios [6]. Other reasons are the effect of fuel type or other emission reduction technologies on (indoor) air quality [7–10], assessing the impact of new legislation on air quality [11, 12], compliance monitoring in emission control areas evaluating the impact on health and well-being [13, 14], etc. All these reasons require information about the emission of pollutants. One way to gain insight into the emissions of ships is through fuel emission inventories obtained by the amounts of sold or consumed fuel combined with emission factors [15–22] or with automatic identification system (AIS) data [23, 24]. An alternative method is to measure or calculate the concentration of emitted pollutants. This can be done with measuring stations at the banks of rivers, in harbours or on the shore [25–27], air sampling [28], (portable) emission measurement systems [29–32], continuous-time monitoring campaigns [33–38], sniffing methods with drones or airplanes [39–44], or dispersion models [12, 45, 46]. Besides the emission of a complex mixture of gaseous and particulate residuals from burnt fuel [17, 47–50], pollutants are also emitted by the loss of lubricant oil through the combustion chamber and the tailpipe [51]. Other sources of pollution

emission are the bunkering process (i.e., supply of fuel to the ship) and the cargo, especially during loading, cleaning, or discharging [52–54].

Most of the time, the crews work inside the wheelhouse or in the engine room. They also eat, relax, and sleep indoors. Therefore, a ship is not only a place where work and daily life come together but also a location where they can be exposed for extensive periods of time to indoor air contaminants. As a result, indoor air quality on board ships has a significant impact on the crew's health and their quality of life. Despite the extensive studies of pollution emitted by ships, there is little information about the indoor air quality on board ships [7, 14, 55, 56]. One can find more literature about indoor air quality inside buildings [57–60]. To gain more insight about the impact of indoor air on the crew's health, a study is performed on a 36-year-old ship that is used for nearshore operations at the Belgian coast. The analysis started with a visual inspection of the ship to identify the locations where the highest risks could be expected. In the selected locations, 4 short-term measurement campaigns have been organized over a period of 2 years. During these campaigns, a large set of environmental parameters such as inorganic (i.e., CO, NO_2, NO, O_3, SO_2, and H_2S) and organic gaseous pollutants (i.e., total volatile organic compounds and several individual organic compounds including polycyclic aromatic hydrocarbons) and particulate matter (i.e., black carbon, PM_1, $PM_{2.5}$, and PM_{10}) have been analysed. Besides time-averaged analyses based on indoor air sampling campaigns followed by measurements in the laboratory, also continuous-time analyses with state-of-the-art reference instruments and lower-cost sensors have been performed in situ.

It is known that environmental parameters outside and inside buildings fluctuate in different frequency ranges, resulting in several types of concentration peaks and valleys in the temporal trends [61, 62]. This contribution demonstrates that also the indoor environmental parameters in a ship show substantial variations over time. Several pollutants have a low background concentration with a superposition of peaks of varying width and height. Such dynamics have been observed for all analysed parameters during all measurement campaigns except for ozone where a higher background with valleys has also been observed. Therefore, the trends can be considered as inherently unstable. This contribution shows that temporal fluctuations in the trends can be used to our advantage because they allow the identification of smaller moments of worse indoor air quality. Such a moment is sometimes characterized by several pollutant peaks that occur simultaneously. The pattern of simultaneously occurring peaks can be unique for a specific pollution source. The frequency and height of the peaks give an indication of the impact of that pollution source on the indoor air quality. A decision-maker who is responsible for improving living and working conditions can directly use this information and take actions to avoid or reduce the reoccurrence of such moments. In principle, he can evaluate the impact of his actions by evaluating the reoccurrence of peaks. Therefore, time-averaged and continuous-time analyses are complementary information sources each giving valuable information about indoor air quality and what can be done to improve it. With this way of working, the emission of exhaust gases is identified as a pollution source that affects indoor air quality on board ship analysed. The outdoor pollutants must enter the ship through the ventilation system. This phenomenon has also been suggested in other studies [7].

2. Materials and Methods

2.1. Selection of Measuring Locations. The 51-metre ship used 2 diesel engines during the measuring campaigns. The main engine is used for propulsion at sea and for manoeuvres in the harbour, while the second engine is used as an auxiliary engine for producing electricity on board. When the ship is alongside the berth, both engines are stopped, and shore current is used instead. While underway, the main and auxiliary engines run simultaneously, but at different loads. Whenever the ship is manned, the ventilation on board is turned on. Outdoor air is sucked inside through the inlet that is situated at the backside of the wheelhouse, a few meters away from the chimney, and then distributed over each compartment on board. For the engine room, a separate powerful ventilation system is used that provided fresh air for the engine's internal combustion. The air inlet for this system is situated at the front side of the chimney directed towards the backside of the wheelhouse. The outlet of the chimney, where exhaust gases are blown into the air, is located higher than the inputs for both ventilation systems.

A mixed team of scientists and members of the crew visited the rooms of the ship in group to find the hotspots where elevated health risks due to indoor air might occur. The team considered several risk-related indicators such as (1) the existence of pollution sources in the room or contact with a more distant source, (2) the type of activity performed in that room (i.e., work or leisure), and (3) the frequency of occupancy of the room by the crew. These location specific properties remained stable during the course of the study. The following locations have been selected for a chemical analysis of the air: the wheelhouse, the engine room, a storage room for solvents behind the engine room, a sleeping cabin closest to the engine room, the mess, and an outdoor shelter on the poop deck.

2.2. Measurement Campaigns on Board Ship. Once the measuring locations have been identified, several measuring campaigns are organized using a variety of analytical methods. Table 1 gives an overview of the campaigns. Some rooms are analysed more in detail while others have been analysed several times. The following methods have been used:

(i) Passive sampling of volatile organic compounds (VOCs): VOCs are collected with Radiello™ diffusive samplers (Istituti Clinici Scientifici Maugeri, Italy) containing an activated charcoal adsorbent cartridge (adsorbing cartridge code 130). After sampling, the VOCs trapped in the sampling cartridge are desorbed with carbon disulfide and then

Table 1: Overview of the measurement campaigns.

Nr.	Period campaign	Location	Analytical technique
1	13/01/2020–24/01/2020	Wheelhouse	Continuous-time: Humlog 20 Time average: Radiello NO_2/SO_2, Radiello VOCs, PDMS PAH
		Engine room	Continuous-time: Humlog 20, CO sensor Time average: Radiello NO_2/SO_2, Radiello VOCs, PDMS PAH
		Storage room	Continuous-time: Humlog 20 Time average: Radiello NO_2/SO_2, Radiello VOCs, PDMS PAH
		Cabin	Continuous-time: Humlog 20, CO sensor, aethalometer, sensor prototype Time average: Radiello NO_2/SO_2, Radiello VOCs, PDMS PAH, canister VOCs
		Mess	Continuous-time: Humlog 20, CO sensor, aethalometer Time average: Radiello NO_2/SO_2, Radiello VOCs, PDMS PAH
		Outdoor shelter	Continuous-time: Humlog 20 Time average: Radiello NO_2/SO_2, Radiello VOCs, PDMS PAH
2	07/09/2020–11/09/2020	Engine room	Continuous-time: sensor prototype
3	23/09/2020–27/11/2020	Wheelhouse	Continuous-time: sensor box, Grimm Time average: Radiello NO_2/SO_2
		Engine room	Continuous-time: sensor prototype Time average: Radiello NO_2/SO_2
4	15/03/2021–18/03/2021	Wheelhouse	Continuous-time: sensor box
		Engine room	Continuous-time: air pointer, sensor box

analysed with gas chromatography coupled to a mass spectrometer (GC-MS) of Agilent Technology, USA, using the appropriate Radiello protocol. Unopened field blanks are analysed to assess possible contamination through the sample collection and analysis process. A full screening of all peaks is performed for compound identification. A set of 29 compounds has been quantified, while the concentrations of the other compounds are compared with the internal standard 2-fluorotoluene, which has the same sensitivity as toluene. Their concentrations are expressed in toluene equivalents

(ii) Passive sampling of nitrogen dioxide and sulfur dioxide: SO_2 and NO_2 are sampled with a Radiello™ cartridge code 166 consisting of microporous polyethylene (PE) coated with triethanolamine (TEA). After exposure, the reagents are extracted from the cartridges and quantified with ion chromatography according to the methods recommended by Radiello. Field blanks are collected and analysed to assess possible contamination through sample collection and analysis process

(iii) Active sampling of polycyclic aromatic hydrocarbons (PAHs): programmable personal air pumps SG 350 (GSA Messgerätebau GmbH, Germany) are used to sample both gaseous pollutants and particulate matter on mixed bed (polydimethylsiloxane (PDMS)/Tenax TA) sorption tubes with a constant sampling flow of 300 mL min^{-1} for 72 hours (1296 L sampling volume). After sampling, the PDMS/Tenax TA sorbent tubes are sealed with end caps and stored under nitrogen atmosphere until analysis. All samples are analysed within 7 days after sampling using an automated thermal desorber TD100-XR™ (Markes International Ltd., UK) coupled to a gas chromatograph (Thermo Trace GC Ultra) equipped with a mass spectrometer (Thermo DSQII, Thermo Fisher Scientific Inc., USA). The parameters, performance, and validation of the method for PAH analysis are described elsewhere [63]

Besides the time-averaged analyses, also continuous-time measurements have been used during the measurement campaigns. These methods provide an insight in the way pollutant concentrations vary over time. The following instruments have been used:

(i) Humlog 20: The Humlog 20 datalogger (E+E Elektronik, Austria) measures the relative humidity (RH), temperature (T), and CO_2. The sampling time is set to 1 minute. In campaign 1, several of these devices have been installed in the selected locations. Since all devices have been calibrated prior to the measurement campaign, it is possible to compare simultaneous measurements in different locations

(ii) Aethalometer: the microAeth®/AE51 is used to monitor the time profile of black carbon concentrations in indoor air

(iii) Grimm: the Grimm 11-D (Aerosol Technik, Germany) particle monitor (particle size range: 0.253–35.15 μm, concentration: 0 μg/m^3-100 mg/m^3, and reproducibility: ±3% for total measuring range) is used to monitor the PM_1, $PM_{2.5}$, and PM_{10} concentration levels inside the rooms. It should be remarked that particulate matter in fresh ship engine exhaust is in the ultrafine particle size range (i.e., 1–400 nm) [64–66], and a large fraction of these particles remain invisible for the instrument. Through coagulation, the particles increase in size over time and become visible to the instrument

(iv) Airpointer: the transportable air quality instrument Airponter® (mlu-recordum Environmental Monitoring Solutions, Austria) equipped with monitoring systems for continuous measuring of NO, NO_x, NO_2, and O_3 concentrations in air is placed and tied up in a room close to the aft deck. Air from the engine room is sucked in the instrument with a sampling tube of about 30 m and measured every minute. Prior to the measurement campaign, the instrument has been calibrated using gas bottles with reference concentration of the target gases and with an ozone generator

(v) Sensor prototype: the first version of the sensor box is based on a commercially available multipurpose data logger (DataTaker DT85, Thermo Fischer Scientific, Australia) that is able to read an array of various analog sensors. To make the system transportable, the datalogger and a series of calibrated sensors have been built in a metal rack. The rack also contains power supplies for the sensors. More information about the system can be found elsewhere [67, 68]. A sampling time of 5 minutes has been used

(vi) Sensor box: a second version of the in-house built sensor box based on a Raspberry Pi 3 Model B+ is able to measure temperature, relative humidity, pressure, CO, NO_2, O_3, NO, H_2S, SO_2, TVOC, PM_1, $PM_{2.5}$, PM_{10}, and position with a sampling time of 3 minutes. These are common pollutants emitted by diesel engines [9, 35] and are also the main pollutants in the determination of emission factors [22, 46]. More information about the sensor box can be found elsewhere [31]

2.3. Benchmark. By comparing the measurements with reference values, it is possible to check whether the pollutant concentrations are acceptable. Legislation imposes such reference values to protect the well-being (e.g., noise, vibration, and CO_2) and health of employers (e.g., gaseous and particulate pollutants). Since the crew works and lives on a ship, the short- and long-term occupational and nonoccupational thresholds must be considered.

Indoor air quality at workplaces is regulated by thresholds imposed by Belgian and European legislation [69–71]. For indoor air quality where persons are exposed to pollutants in a nonworking context (e.g., citizens in a public building, during leisure time, and residents in their homes), the thresholds are more severe. The thresholds are about 2 (i.e., O_3) to 800 (i.e., NO_2) times lower than their occupational equivalents. This study uses the thresholds of the Flemish Indoor Air Quality Decree to evaluate nonoccupational indoor air [72].

In addition to the formal reference values imposed by legislation, measurements can also be compared with a region where a community perceives the air quality as "good" or "bad." Outdoor air from a large city is usually considered as worse than, for example, rural areas. Although an air quality study of an urban and a rural region in Belgium suggests that the rural area is indeed somewhat better, such claims are harder to substantiate than one might suspect [62]. The city of Brussels, Belgium, has been selected as benchmark because it is the largest city in Belgium. In addition, the national monitoring stations of the Belgian Interregional Environmental Agency (IRCEL-CELINE) measurement network cover in that city the largest range of environmental parameters that are measured simultaneously. The data from stations 41R001 in Saint-Jean Molenbeek and 41B006 close to the European parliament are publicly available [73]. An alternative region where air quality is considered as good is a maritime environment or a coast city such as De Haan, Belgium, that is far from the influence of industrial activity [74]. The reference values are defined as the average concentrations at the given location of the same period as the measurement campaign.

3. Results

Prior to the continuous-time analyses, the time-averaged chemical analyses of several gaseous pollutants performed during campaign 1 are presented first. Table 2 gives an overview of the Radiello analyses at the different locations. The measured concentrations of the outdoor pollutants are systematically lower than the indoor concentrations. The reason for this is that the shelter slightly shields the outside location, so the exhaust gases reach the measurement location mainly through the slower diffusion process. This gives the exhaust gases more time to dilute. At the same time, convection can bring the exhaust gases with limited dilution directly to the ventilation inlet that is in the neighbourhood of the funnel so that pollutants penetrate the ship's castle. Another study also found that the concentration of exhaust gases was higher indoors than outdoors [7]. The continuous-time outdoor analysis of toluene in Brussels shows a background concentration that is usually below 2 μg/m^3 with tall but narrow peaks that often exceeds 100 μg/m^3. The average toluene concentration in Brussels during the period of the measurement campaign is 14 μg/m^3 and is higher than its background concentration but lower than the peak maxima. The reported toluene concentration in the ship's rooms is between 8 and 30 μg/m^3, but it is not clear if the average concentrations in Table 2 are caused (1) by a steady background concentration or (2) by a different frequency of peaks on a low background concentration. The uncertainty about the pattern in the temporal trend complicates the comparison

Table 2: Chemical analysis of volatile organic compounds (VOC) in $\mu g/m^3$, some inorganic gases in $\mu g/m^3$, and polyaromatic hydrocarbons (PAH) in ng/m^3 performed in the 6 locations during measurement campaign 1 using diffusion tubes. The values in bold are semiquantitative analyses and expressed as toluene-equivalent concentrations. The columns are ranked according to decreasing TVOC content. The organic compounds are arranged according to increasing number of C-atoms in the parent chain.

Radiello VOC ($\mu g/m^3$)	Storage room	Engine room	Cabin	Mess	Wheelhouse	Outdoor
TVOC	1274	554	328	199	151	32.3
Trichloromethane	0.32	<0.22	0.50	0.27	<0.22	<0.20
Tetrachloromethane	0.46	0.47	0.46	0.51	0.50	0.47
1,2-Dichloroethane	4.92	0.24	0.23	<0.22	<0.22	<0.19
cis-1,2-Dichloroethene	7.72	0.31	<0.23	0.36	<0.24	<0.21
1,1,1-Trichloroethane	<0.27	0.51	<0.27	<0.27	<0.27	<0.24
1,1,2-Trichloroethane	1.01	0.35	0.52	<0.27	<0.27	<0.24
Vinyl acetate	0.30	<0.28	<0.27	<0.28	<0.28	<0.25
n-Butyl acetate	4.01	<0.92	<0.91	<0.92	<0.93	<0.82
Acetone	42.26	9.80	8.55	11.01	8.00	1.05
Pentane	37.02	10.94	26.68	15.45	17.41	2.53
Hexane	22.28	7.47	14.96	8.38	9.62	1.62
3-Methyl hexane	**18.99**					
Cyclohexane	24.51	9.20	19.64	10.00	10.72	1.46
Methyl cyclohexane	**51.53**	**16.59**	**23.23**	**11.04**	**12.03**	
Benzene	5.70	3.04	5.05	3.23	3.31	1.21
Toluene	32.54	11.69	16.55	8.72	8.33	2.72
m+p-Xylene	49.11	21.30	22.72	9.48	8.80	3.92
o-Oylene	19.23	9.06	9.28	3.86	3.45	1.55
1,3,5-Trimethylbenzene	5.23	2.03	1.48	0.58	0.49	<0.85
1,2,4-Trimethylbenzene	40.08	14.35	9.40	3.58	2.84	1.54
1,2,3-Trimethylbenzene	14.34	4.75	2.52	<1.11	<1.12	<0.99
Ethylbenzene	17.30	7.01	7.31	3.25	2.99	1.34
p-Diethylbenzene	12.04	4.66	2.43	0.80	0.62	0.38
o,m,p-Ethyltoluene	**42.47**		**10.98**			
Cumene	2.35	1.43	1.04	<0.95	<0.97	<0.85
Heptane	69.73	17.13	15.76	7.53	7.82	1.46
n-Octane	19.08	10.76	9.69	4.56	4.65	1.75
n-Nonane	67.79	21.47	11.12	4.76	4.47	2.63
n-Decane	162.46	59.49	12.63	6.56	4.43	3.40
Limonene	6.80	<1.28	2.85	45.01	10.64	<1.15
Alpha-pinene	12.14	<1.04	<1.03	<1.04	<1.06	<0.93
Decahydronaphthalene	**21.62**	**10.14**	**0.00**			
Undecane	**402.6**		**39.55**			
Dodecane	**623.4**	**391.1**	**178.1**	**180.9**	**135.4**	**56.16**
Tetradecane	**12.78**	**9.63**	**9.84**	**11.78**	**9.98**	**7.26**
Hexadecane	**4.24**	**5.00**	**4.79**	**5.76**	**5.44**	**5.86**
Radiello NO_2/SO_2 ($\mu g/m^3$)	Storage room	Engine room	Cabin	Mess	Wheelhouse	Outdoor
NO_2	4.86	14.57	15.36	13.22	15.01	2.00
SO_2	<2.6	<2.6	<2.6	<2.6	<2.6	<2.6
PAH analysis (ng/m^3)	Storage room	Engine room	Cabin	Mess	Bridge	Outdoor
Naphthalene	—	179.9	169.9	120.6	125.2	84.7
Acenaphthene	—	47.7	11.0	15.4	9.2	0.5
Acenaphthylene	—	18.4	9.0	12.4	9.9	0.6
Fluorene	—	1.8	4.4	5.9	6.3	3.4

Table 2: Continued.

Phenanthrene	—	11.6	6.7	6.5	11.2	4.4
Anthracene	—	6.3	3.1	2.5	12.3	2.1
Fluoranthene	—	1.1	0.7	0.3	0.8	1.0
Pyrene	—	1.4	0.6	0.2	0.8	0.8
Benzo(a)anthracene	—	<0.02	<0.02	<0.02	<0.02	0.2
Chrysene	—	<0.04	<0.04	<0.04	<0.04	0.2
Benzo(b)fluoranthene	—	<0.04	<0.04	<0.04	<0.04	<0.04
Benzo(k)fluoranthene	—	<0.15	<0.15	<0.15	<0.15	<0.15
Benzo(a)pyrene	—	<0.01	0.2	<0.01	<0.01	2.5
Indeno(1,2,3,-cd)pyrene	—	<0.01	<0.01	<0.01	<0.01	<0.01
Benzo(g,h,i)perylene	—	<0.07	<0.07	<0.07	<0.07	<0.07

between the measured concentrations and the benchmark. When the volatile organic compounds are examined with Radiello tubes and with the canister method (see Table S-I in supplementary material), it appears that the canister method identifies more pollutants. Since every pollutant contributes to the general indoor air quality, the overall situation gets worse as more pollutants are identified. Besides the more general observations, the list below gives an overview of more specific observations and comparisons with the benchmark.

(i) Inorganic gases: the average indoor NO_2 concentration on board ship ranges from 5 to 15 $\mu g/m^3$, which is higher than the outdoor location on the ship ($2\,\mu g/m^3$). For SO_2, the concentrations are below the detection limit of the Radiello method, thus lower than $2.6\,\mu g/m^3$. When compared to the Flemish nonoccupational thresholds (target value NO_2: $20\,\mu g/m^3$; intervention value NO_2: $40\,\mu g/m^3$), the indoor air quality assessed during this sampling period can be considered as safe. That legislation does not include a threshold value for SO_2. During the same period, the Brussels' outdoor air contains $25 \pm 16\,\mu g/m^3$ and $36 \pm 24\,\mu g/m^3$ NO_2 at the stations 41R001 and 41B006, respectively. This means that for this pollutant, the indoor air on board ship is better than the benchmark. The SO_2 concentration at station 41R001 contained $2.0 \pm 1.5\,\mu g/m^3$ SO_2 (i.e., below the detection limit of Radiello tubes)

(ii) Organic gases: from the quantitatively assessed compounds presented in Table 2, the organic compounds in the highest concentrations are n-decane (storage room and engine room), limonene (mess), pentane (cabin and wheelhouse), and m+p xylene (outdoor). This means that there is no single dominating organic pollutant in the ship and that the makeup of the mixture is location dependent. For benzene, the 8-hour time-weighted average occupational threshold is $3250\,\mu g/m^3$ [70, 75]. The highest benzene concentration that has been measured in the ship is $5.7\,\mu g/m^3$ (i.e., storage room). If we only look at benzene, the ship can be considered as a safe workplace. The Flemish nonoccupational intervention value for benzene in indoor air is equal to a minimum of $0.4\,\mu g/m^3$ or to the outdoor concentration if this is higher than the minimum value. All indoor concentrations are higher than the outdoor concentration (i.e., $1.21\,\mu g/m^3$), meaning that the indoor air quality is not safe for nonworking conditions. For the outdoor air of Brussels at station 41B006, the BTEX compounds benzene, toluene, ethylbenzene, and ortho-xylene and the mixture of meta and paraxylene are $0.5 \pm 0.3\,\mu g/m^3$, $14 \pm 20\,\mu g/m^3$, $3 \pm 2.3\,\mu g/m^3$, $3 \pm 2\,\mu g/m^3$, and $7 \pm 5\,\mu g/m^3$, respectively. For a number of gases, the indoor concentrations at all locations are higher than for the outdoor air of Brussels (e.g., benzene, ethylbenzene, and ortho-xylene). For other pollutants, only in a few locations the concentrations exceed the corresponding city value (e.g., toluene in the storage room and in the cabin). This means that some pollutants give the impression that the indoor air quality on the ship is better than air quality of a large city and in other cases not. The comparison with the benchmark gives an ambiguous picture about the indoor air quality in the ship

(iii) Total volatile organic compounds (TVOC): Table 2 contains a long list of detected organic compounds that exist in air in low concentrations. The TVOC results summarized in Table 2 suggest that they are more than 10 times higher than the concentration of the individual compounds. Using the ALARA-principle (i.e., as low as reasonably achievable), it can be argued that a room with a lower TVOC concentration is supposed to be healthier than one with a higher TVOC concentration no matter what the threshold is. Using that principle, it is possible to rank the analysed locations from worse to better air quality: storage room > engine room > cabin > mess > wheelhouse > outdoor. This ranking is also used to organize the measurements in Table 2. The high TVOC concentration in the engine room and in the storage room is most probably due to the evaporation of fuel that escapes from

the engine and from solvents kept in bottles. When compared with the intervention value of the Flemish Indoor Air Quality Decree for nonoccupational conditions, only the storage room exceeds the intervention value (<1000 $\mu g/m^3$) while the engine room and cabin exceed the TVOC guideline value (<300 $\mu g/m^3$). The number of analysed pollutants becomes larger when air is sampled with canisters (see Table S-I in the supplementary material). The analyses suggest that as more organic compounds are identified, the indoor air quality becomes worse because it increases the TVOC content. Therefore, organic compounds invisible to the analytic method affect the air quality assessment

(iv) Polycyclic aromatic hydrocarbons (PAH): of all PAHs present as gas or associated with particles, naphthalene is the most dominant species with an indoor concentration in the range of 121–180 ng/m^3. This is somewhat higher than the outdoor concentration underneath the shelter (i.e., 85 ng/m^3). For naphthalene, the concentrations are well below occupational thresholds (i.e., average concentration of 53 mg/m^3 for an 8-hour exposure in Belgium [69]) and below the nonoccupational Flemish intervention value of 31 $\mu g/m^3$ [72]. It is even below EPA's daily reference concentration for inhalation (RfC) of 3 $\mu g/m^3$ [76]. Unfortunately, there is no PAH data available from the reference stations in Brussels. However, it can be compared with PAH analyses performed in Flanders (Belgium) some years ago where the background levels of PAHs in ambient air are reported to be 0.02–1.2 ng/m^3 in rural areas and 0.15–19.3 ng/m^3 in urban areas. Concentrations up to 114 ng/m^3 were observed in the vicinity of petroleum industry [74, 77, 78]. Therefore, the indoor air of the ship is comparable with the outdoor air of larger cities and industrial zones. Naphthalene and phenanthrene have also been observed in the emission of other sea going vessels [36]

3.1. Engine Room. The sailing period during measurement campaign 4 started on 15/3/2021 at 10 : 00 and ended on 16/3/2021 at 21 : 30. The moments prior and after that period, the ship is moored in port. The time series measured by the Airpointer and shown in Figure 1 demonstrates that the trends of the pollutant concentrations are highly variable and that NO and NO_2 show narrow peaks with elevated concentration. For O_3, valleys have been detected on a larger background concentration. The following striking observations have been made:

(i) Tall but narrow peaks and valleys: during the sailing period of 1.48 days, the Airpointer detected 28 narrow, tall NO/NO_2 peaks (see Figure 1). The width of these peaks as defined at the baseline is in the range of 2-25 minutes (average ± standard deviation: 8 ± 6 minutes). For O_3, valleys with a width of 2-24 minutes (average ± standard deviation: 12 ± 7 minutes) have been detected. Both the ship and the outdoor air in Brussels at measuring station 41R001 are characterized by NO_2 trends with peaks, but the peaks in the ship are about a factor 2 higher. For NO, the peaks in the engine room are about a factor 10 higher when compared to Brussels. The average ozone concentrations for the ship and city are similar. This analysis suggests that at some occasions, the air quality in the engine room is worse than the outdoor air in Brussels

(ii) Relationship between peaks: at several occasions, the peaks of NO_2 and NO occur simultaneously. This suggests that they are caused by the same pollution source. In most situations, the peak maximum of NO is higher than that of the corresponding NO_2 peak. Since the NO_2/NO ratio varies between 0.16 and 1.5 while sailing, the source appears to generate a variable mixture of pollutants. When NO and/or NO_2 peaks occur, a narrow O_3 valley with a delay of 1 to 9 minutes is systematically observed. A sudden NO peak creates a temporary and localised situation with an excess of NO, and this shifts the reaction $NO + O_3 \rightarrow NO_2 + O_2$ [79, 80] to the right. The chemical coupling between O_3 and NO/NO_x as described by the fast reaction is also responsible for the so-called "ozone paradox" causing lower ozone concentrations in cities than in rural areas because of the higher amounts of NO_x in cities

(iii) Total duration of peaks vs. health: workplace exposure limits are usually described by 2 threshold values. The first threshold value is the short-term exposure limit (STEL: exposure to a time-weighted average concentration of a substance during the previous 15 minutes thought not to be injurious to health). The second threshold value is the long-term exposure limit (LTEL also known as TWA: time-weighted average concentration of a substance over an 8-hour period thought not to be injurious). Both limits use average concentrations to evaluate indoor air. To apply such an evaluation on continuous-time measurements, the time series must be treated with a right aligned moving average with a window width of 15 minutes or 8 hours, respectively. Then, each data point can be compared with the corresponding STEL (e.g., for Belgium NO_2: 5 ppm; NO: 2 ppm, O_3: 0.1 ppm) or LTEL (e.g., for Belgium NO_2: 3 ppm; NO and O_3 not defined). All data points for all pollutants in Figure 1 are below the given thresholds, and the working conditions in the engine room can be considered as safe. However, the moving averages used to calculate the values that can be compared with the STEL and LTEL suppress or even completely remove the narrow peaks with high concentration.

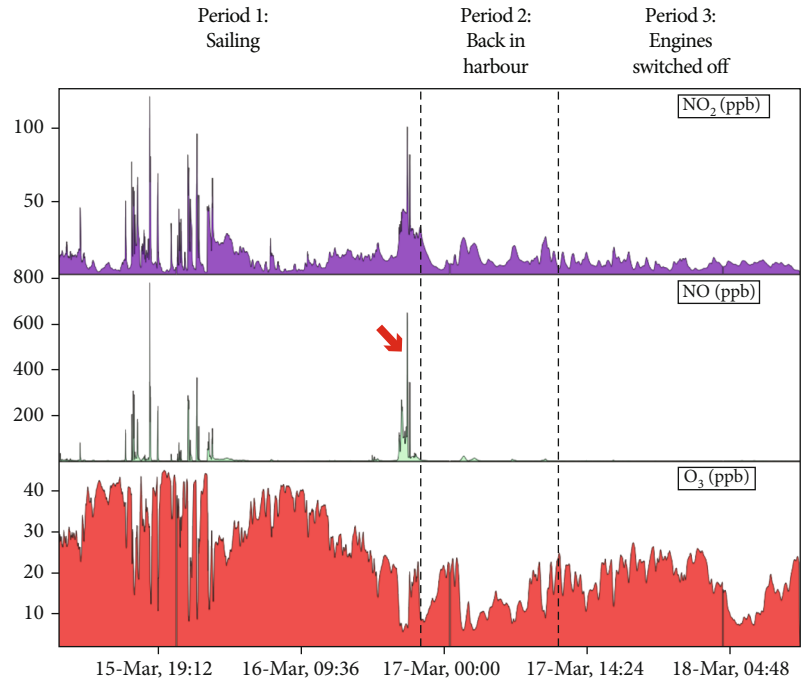

Figure 1: Time series plots of NO_2, NO, and O_3 of the engine room expressed in ppb as determined by the Airpointer during measurement campaign 4.

For NO_2, the nonoccupational threshold is more severe (i.e., 10.64 ppb) suggesting that the occurrence of the small peaks above 40 ppb do have an effect on human health. The total exposure time to NO/NO_2 events is 3.75 hours, which is about 11% of the sailing period but only 5% of the total duration of the measurement campaign. While these peaks have little effect on the current methods to assess air quality, the total exposure to such peaks cannot be considered as negligible. Therefore, the peaks may have a greater impact on the health of the crew than these methods suggest. Moreover, the relatively short duration of these events has a limited effect on the mean concentration determined by time-averaged analysis methods using diffusion tubes

In parallel to the Airpointer, the same environment is also analysed with the sensor box that entails a large set of sensors. All meaningful trends are shown in Figure 2. For NO, NO_2, and O_3, similar observations could be made as the previous analysis using the data of the Airpointer (Figure 1). The average concentration for CO, NO_2, O_3, and NO in the engine room is 220 ± 66 ppb, 70 ± 16 ppb, 24 ± 8 ppb, and 7 ± 10 ppb, respectively. These concentrations are similar to the outdoor air in Brussels, except for NO_2 which is higher than the benchmark. The $PM_{2.5}$ concentration ($8 \pm 6\,\mu g/m^3$) in the engine room is similar to that of outdoor air in Brussels ($10 \pm 7\,\mu g/m^3$). It is striking how all measured parameters fluctuate. Based on the ship's activity, the time series have been divided in 3 periods (sailing, back in the harbour, and engines switched off). These periods distinguish themselves by the absence or presence of peaks or by different peak widths. In addition, all measured environmental parameters show characteristic features and trends. Most of them consist of a slowly fluctuating background with well-defined peaks on top of that background. From the additional measurements, the following observations have been made:

(i) Pattern of simultaneously occurring peaks: at some occasions, a pattern of simultaneously occurring peaks can be observed. This can be observed for the largest NO peak in the time series (see red arrow in NO graph in Figures 1 and 2) where peaks of NO, NO_2, CO_2, CO, and TVOC coincide. Only for a few occasions during period 1, there is also a correlation with the narrow peaks of PM_1, $PM_{2.5}$, and PM_{10}. A correlation with O_3 could not be observed. The pattern of coinciding peaks suggests that they originate from the same pollution source. Since this combination of pollutants is also found in exhaust gas emitted by ships [35], this pattern can be associated with exhaust gas entering the engine room. The coincidence of peaks becomes harder to notice when the NO/NO_2 peaks become smaller. Another reason why the coincidence is harder to identify is when small peaks are superposed on a high background. For CO_2, the peaks have a height of 10–20 ppm on top of a background level of around 546 ppm (e.g., blue arrow in the CO_2 graph of Figure 2). The peaks cannot always be distinguished from the high frequency and random fluctuating noise around the average background concentration. Such peaks

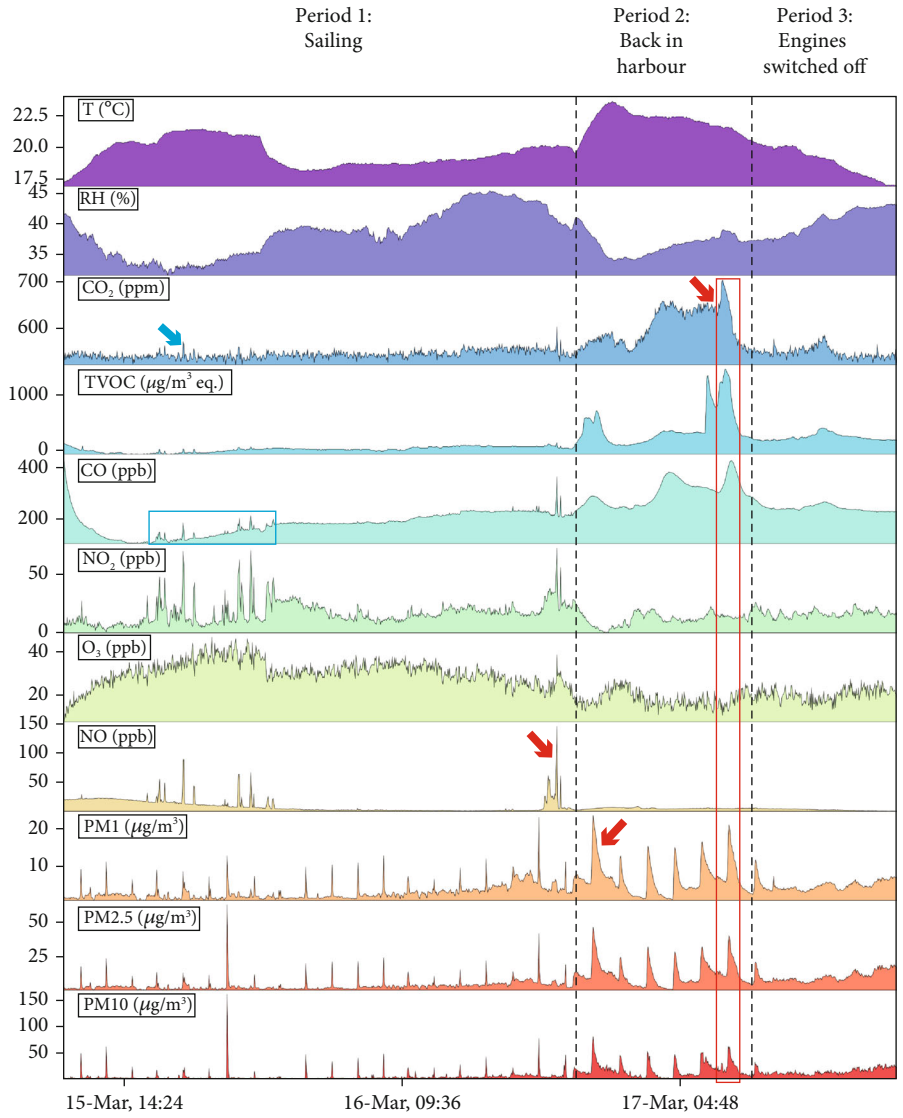

Figure 2: Time series obtained with the sensor box performed in parallel with the Airpointer in the engine room shown in Figure 1 (measurement campaign 4). Based on the ship's activity, the time series has been divided in 3 consecutive periods: period 1 is while sailing, period 2 from March 16 at 21 : 30 and end on March 17 at 11 : 30 is when the ship is back in the harbour, and period 3 is when the engines have been switched off.

may be confused with an outlier, or outliers may be falsely considered as a peak. In addition, the CO_2 graph is dominated by the large peak of 705 ppm on March 17 at 7 : 48 in period 2 (i.e., red arrow in CO_2 graph of Figure 2) so that the small peaks in period 1 are even more suppressed. Also, the CO peaks that coincide with the NO/NO_2 peaks (e.g., blue rectangle in Figure 2) are small and on top of a high background. They can easily be missed, especially when they consist of 1 data point. The coincidence of such peaks with that of other pollutants helps to identify them as peaks. The pattern of coinciding tall but narrow peaks does not occur in period 3 when the ship is moored in the harbour and the engines are switched off, yet another argument that the source of these peaks is the engine

(ii) Pattern of consecutive peaks: the large CO_2 peak at the red arrow in Figure 2 is followed by a peak of TVOC (at 8 : 00), PM (at 8 : 15), and CO (at 8 : 24). Although there is no instantaneous coincidence, the series of peaks in the red rectangle in Figure 2 suggest some causal correlation

(iii) Smaller and broader peaks: period 2 in Figure 2 is the moment the ship arrives back in the harbour. It consists of 7 sharp but broad PM peaks (arrow in PM_1 graph) and of several overlapping TVOC, CO, and CO_2 peaks and some low but broader NO_2 peaks. Since the broad peaks of CO_2, TVOC, and CO are overlapping, it is not straightforward to determine their width, but they appear to be wider than 60 minutes. These broad peaks appear

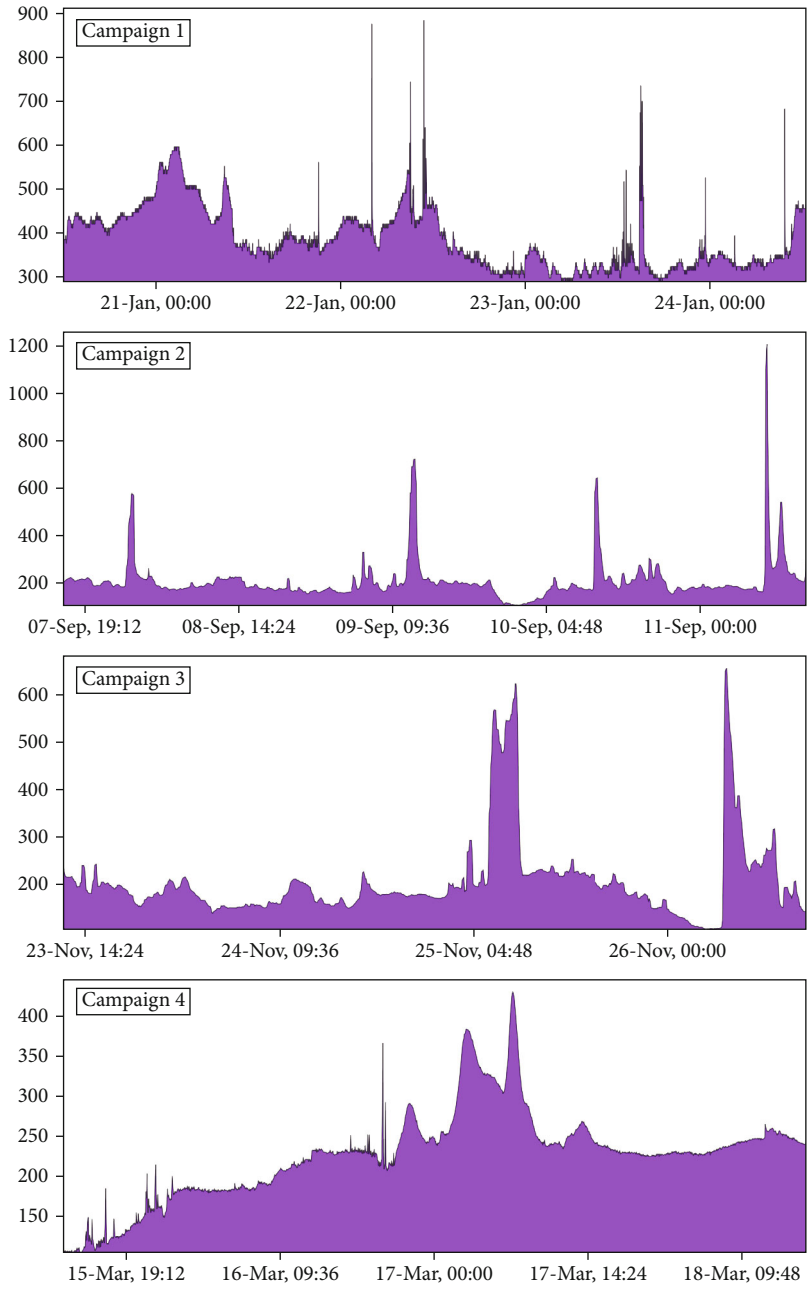

Figure 3: CO concentration trends in the engine room during the 4 measurement campaigns.

to be caused by a different (behaviour of the) pollution source than the tall peaks occurring in period 1

(iv) Regular periodicity in PM peaks: the position of many PM peaks in periods 1 and 2 appears to show some regularity with a median period of 108 minutes between them. The events are more prominent in the PM_{10} signal than in the PM_1 signal. It is unclear what is causing this regularity, but it might be caused by a pump or generator in the engine room switching on at regular occasions. The sudden increase in vibration may cause resuspension of dust. This regularity has not been observed in the wheelhouse, suggesting that this is a local phenomenon inside the engine room. Also in campaign 3, a regularity in the tall PM peaks has been observed in the engine room with an initial periodicity of 108 minutes and in a later stage of 95 minutes

The example in Figure 3 about the CO concentration in the engine room illustrates that the strong fluctuations of the environmental conditions are unique for each measurement campaign. All show a slower fluctuating background with well-defined peaks on top. In some cases, these peaks are tall;

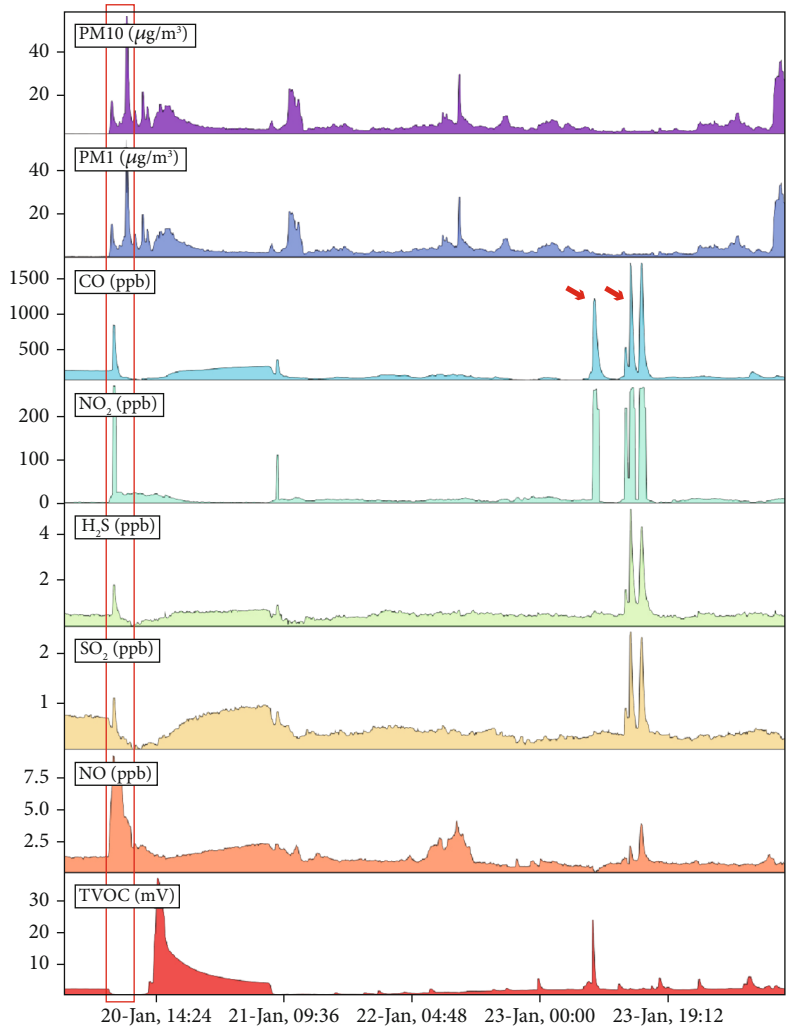

Figure 4: Concentration of gases and particulate matter monitored in the cabin during campaign 1 as measured with the sensor prototype.

at other moments, these peaks are broader. The 4 time series illustrate the inherent instability of the environmental conditions over time.

3.2. Cabin. The indoor air quality of the cabin closest to the engine room has been analysed during measurement campaign 1. It is also close to the outside door that gives onto the poop deck and to the door to enter the engine room. The cabin has a simple beam-shaped volume (2.5 m × 4 m with a height of 2.5 m) with no windows and 1 door. During the journey, the door is always closed. Air is entering the cabin through the ventilation system and escapes through the grid at the bottom of the door. The cabin contained several measuring devices while it is occupied by 1 crewmember. Figure 4 suggests that the concentration of pollutants fluctuates and that high peaks occur at several occasions. Several pollutants show peaks at the same moments. On top of these general observations, the following specific issues have been noticed as well:

(i) Human presence: there has only been human presence in the cabin during daytime to check the measuring devices and to update the logbook and during the night to sleep. The CO_2 peaks due to human presence are obvious in Figure 5 and are in the range of 140–350 ppm on top of the background concentration. The relative humidity has corresponding peaks with an increase of 1–5%. For temperature, a subtle jump of ca. 0.2-0.9°C is often noticed so that the room is warmer after the RH/CO_2 peak than before. In some cases, temperature peaks of 0.2°C are observed on top of that jump. Due to the subtlety of the T and RH changes, this pattern might easily be missed. This means that humans act as a source of variation with a CO_2-RH-T pattern (see Figure 5(b)) where as expected the change in CO_2 is the dominant peak. The CO_2 concentration never reached more than 917 ppm because of the continuous supply of outdoor air in the room

(ii) Heating: after a sudden drop in RH starting on January 21 at 7 : 30 due to the opening of the cabin's door followed by a CO_2-RH-T peak due to human

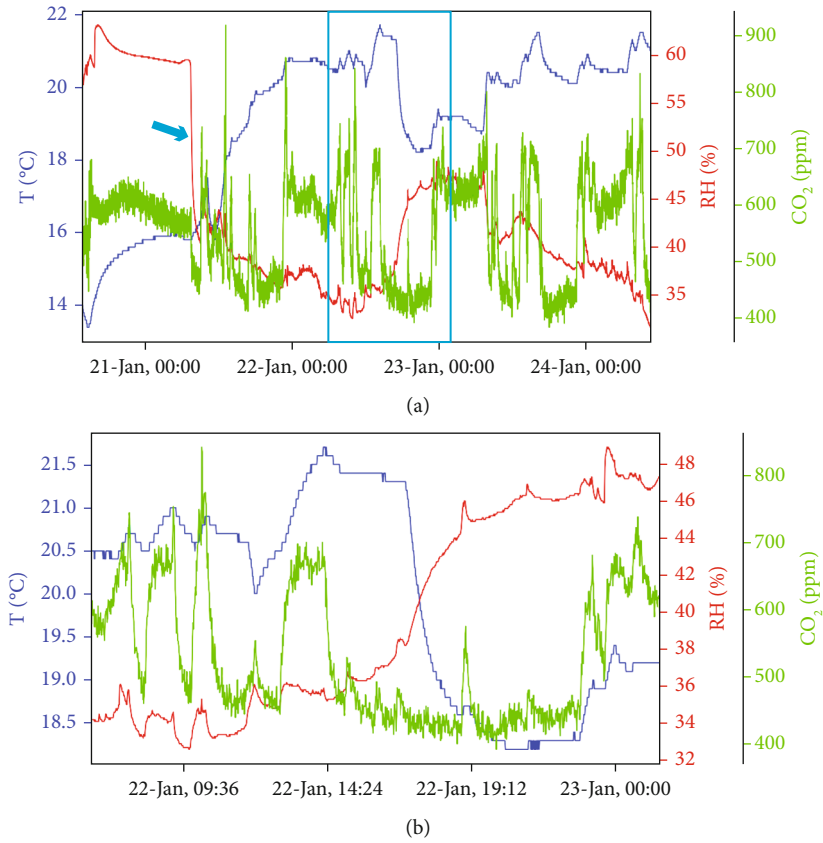

Figure 5: Temperature, relative humidity, and CO_2 measurements with Humlog 20 in the cabin during measurement campaign 1. (a) Overview of the complete measurement campaign with average conditions $19 \pm 2^{\circ}C$, $44 \pm 9\%$, and 560 ± 90 ppm. (b) Detail of the campaign showing the correlation between CO_2, RH, and T due to human presence.

presence, the temperature steadily rises from 16°C to 20.8°C while the RH drops from 42.7% down to 37% from January 21, 12:00 to midnight. The ventilation system that has been switched on takes cold outdoor air ($6 \pm 2^{\circ}C$, $88 \pm 5\%$, and 490 ± 24 ppm) and heats it up to $19 \pm 2^{\circ}C$. Although there is a clear difference in relative humidity between cabin and other indoor spaces on one hand and outdoor air on the other hand, that difference becomes smaller when the moisture content is expressed in absolute humidity in g/m^3. A similar absolute humidity between cabin, the other indoor measuring locations, and outdoor air can be explained when all measured locations are in contact with each other and when the ventilation system only heats the air but does not control the humidity. It does also explain the anticorrelation between RH and T trends observed in the indoor locations

(iii) Bunkering (i.e., supply of fuel to the ship): the day before departure on January 20, the ship has been moved in the harbour for bunkering. This displacement can be seen by the NO_2-CO-CO_2-NO-PM peak at 8:00–8:30 inside the cabin (see red rectangle in Figure 4). The bunkering started at around 12:00. During that operation, all engines and also the ventilation systems are switched off. After bunkering, a large TVOC peak that starts at 14:00 and reaches a maximum at 14:35 can be observed. The TVOC peak slowly decays throughout the rest of the day. This observation suggests that certain peaks in the time series can be attributed to specific events

(iv) Exhaust gas peaks: on January 23, 4 high CO and NO_2 peaks and H_2S/SO_2 peaks with a maximum at around 5 ppb with a width of 20 minutes up to 1 hour have been measured in the cabin (see arrows in Figure 4). At these moments, the engines of the ship and the ventilation of the engine room are switched off and fire drills take place. The ventilation of the ship's castle remained operational. During the exercise, a diesel engine on deck has been switched on to refill the air cylinders for the breathing apparatus and these moments resulted in CO-NO_2-NO peaks in the cabin. No accompanying peaks of particulate matter or black carbon have been observed (see Figure 4). The exhaust gases of that engine must have entered the ventilation inlet of the ship's castle and dispersed over the rooms. This phenomenon could take place because that day it has been almost wind still. This observation

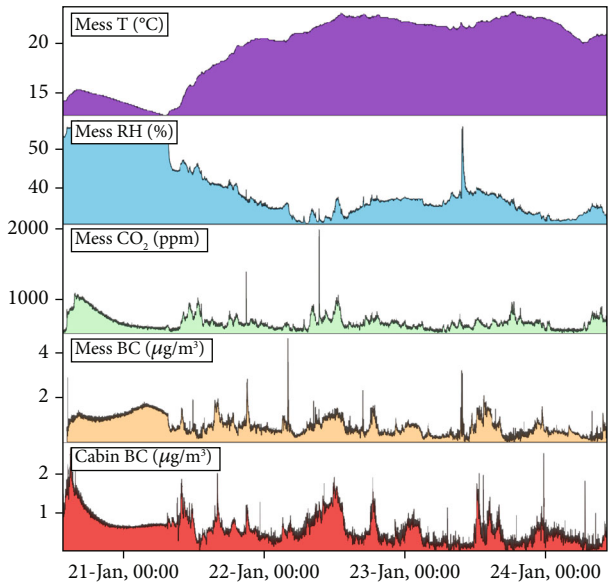

Figure 6: Environmental conditions during campaign 1 in the mess, including the black carbon (BC) concentration of the mess and of the cabin as measured with an aethalometer.

shows that outdoor exhaust gases result in peaks of CO-NO_2-NO in indoor air. It also shows that outdoor pollution sources easily penetrate the accommodations of the ship through the ventilation system. This means that outdoor pollution sources affect the indoor air quality

3.3. Mess. The mess is where the crew meets for meals in the morning, afternoon, and evening. This means that at certain moments of the day, the room is crowded. The air inside the mess can mix with the air of the corridor because the door is usually open. From the preparation of the departure onwards on January 21 at 7 : 30, the trends of relative humidity, CO_2, and black carbon (BC) start to fluctuate more intensely (see Figure 6). Moreover, the following striking issues have been identified:

(i) Human presence: the CO_2 trends in Figure 6 contain several peaks with maxima in the morning at the start of the working day, at noon, and in the early evening. They correspond to the moments that the crews eat. The CO_2 peaks are higher than the values for the cabin (shown in Figure 5) because of the higher number of people

(ii) Black carbon: black carbon is formed by incomplete combustion of fuel and has been monitored in the mess in parallel with the cabin (see Figure 6). The time series of the mess contain 2 large spikes with only 1 data point. They are considered as instrumental errors and have been removed. Even if these spikes would have a physical meaning, it is still advantageous to remove them because it improves the readability of the overall pattern. The remaining spikes consist of at least 2 data points and are for that reason not removed. Despite the fact that both rooms are separated by a corridor, several doors, and 2 stairwells, the trends in Figure 6 show some similarities from the departure of the ship onwards. This suggests that the exhaust gases penetrate deep into the ship, which can only be explained when pollutants are distributed by the ventilation system. The average black carbon concentration in the mess and in the cabin is $0.8 \pm 0.5\,\mu g/m^3$ and $0.6 \pm 0.4\,\mu g/m^3$, respectively, which is higher than the marine background level of about $0.2\,\mu g/m^3$ [5]. The black carbon trends of both locations do show some broad peaks at the same moment. However, a scatter plot does not show an obvious correlation between the 2 locations. The average concentration of black carbon for the same period in Brussels (station 41R001 in Saint-Jean Molenbeek) is $0.5 \pm 0.3\,\mu g/m^3$ suggesting that the indoor air of the ship assessed during this measurement campaign is similar to outdoor air in Brussels. The 4 large NO_2-CO peaks detected in the cabin (see Figure 4) and caused by the diesel engine on deck are not accompanied by BC peaks

(iii) Spatiotemporal variations: Figures 5 and 6 show the dynamics of temperature, relative humidity, and CO_2 of the different rooms in the ship for the same period. The trends are substantially different. When comparing the measurements of the 6 locations, none of them show much similarity. This indicates that the parameters not only vary in time but also in space. The ventilation system is not able to keep the environmental conditions constant in the ship's castle. At the same time, the effect of large events as switching on the ventilation system can be seen in all the rooms analysed. The relative humidity in both mess and cabin starts to drop at the same moment while the temperature starts to increase gradually

3.4. Wheelhouse. As in the other locations, the temperature in the wheelhouse is not constant. During campaign 1, it fluctuated between 8.4°C and 17.9°C. The wheelhouse' doors to the outside are opened when the crew needs to enter or exit or when communication with others outside the wheelhouse is needed during manoeuvres. Therefore, the indoor temperature can severely drop. The lowest temperature is reached on January 21 at 7 : 36 AM. This is the start of the working day prior to departure. The measurement campaigns performed in that location also show that the concentration of the pollutants strongly fluctuates (see Figure 7). Some pollutants show peaks at the same moment, suggesting that the same source emits multiple pollutants. The occurrence of peaks must be caused by a source that switches between 2 states (pollution source emits large amounts of pollutants vs. source is less active, wind blows outdoor pollution towards ventilation inlet vs. wind blows pollution away

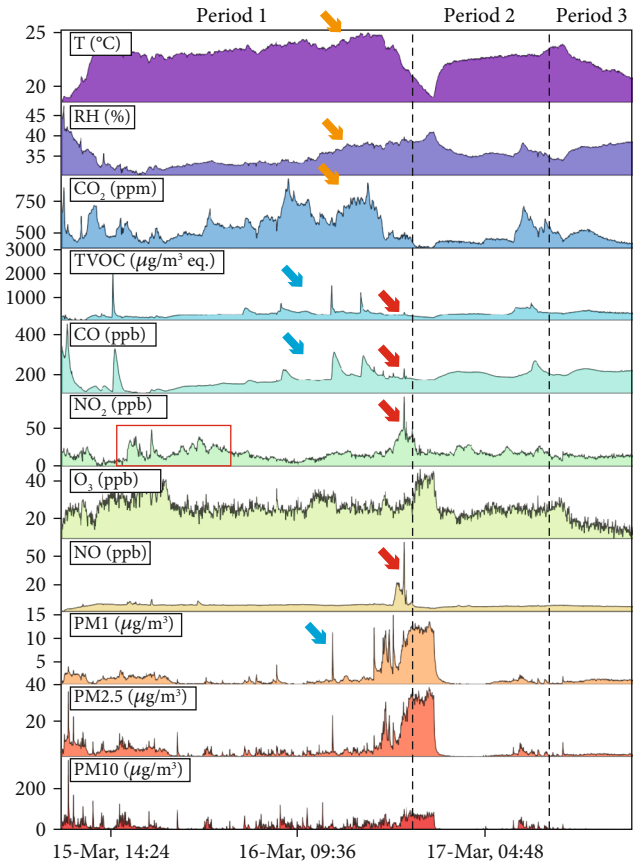

Figure 7: Time series obtained with the sensor box performed simultaneously with the Airpointer in the engine room (measurement campaign 4).

from inlet). More specific observations are summarized below:

(i) Correlation between peaks: although isolated peaks of, for example, CO_2, CO, or NO_2 do occur in the time series, at other moments, CO_2-RH-T peak correlations are found (i.e., orange arrows in Figure 7 show a typical hard to see correlation due to human presence). Peaks showing such correlation correspond with warm, moist air rich in CO_2. At other moments, NO-NO_2-CO-TVOC peak correlations can be observed (i.e., red arrows in Figure 7). At regular occasions, a correlation between CO and TVOC is found, which is sometimes preceded by a PM peak (i.e., blue arrow in Figure 7). The correlation between peaks in the wheelhouse is more complex than in the engine room where human presence and opening/closing doors add an extra layer of complexity in the strong fluctuations in the trends

(ii) Correlation between locations: the environmental situation in the engine room and the wheelhouse during campaign 4 while sailing and with active ventilation is not the same. However, some features in both time series are clearly correlated. For example, the transition from period 1 to period 2 goes along with an increase in temperature in the engine room and a drop in temperature in the wheelhouse. For the NO_X trends of both locations (wheelhouse: detail of the red rectangle in Figure 7 is shown in Figure 8; engine room: trend of the same period is also shown in Figure 8), an obvious correlation can be seen at some moments, while at other moments in only one location, a clear feature can be seen. The marked features in Figure 8 illustrate this distinction. Feature 1 is an example of a peak that is only detected in the wheelhouse. Feature 2 occurs at both locations and can only be explained if it originates from the same pollution source. Feature 3 only occurs in the engine room. Feature 4 occurs at both locations, but the peak in the wheelhouse is broader. This illustrates that the distribution of pollutants in and around a ship is not homogeneous. The NO_2 is a typical exhaust gas, and the funnel on the ship can be considered as a point source. The dispersion of the exhaust gases around that point depends on the distance from the funnel but also from the wind direction relative to the motion of the ship. The inlet of the ventilation for the engine room and for the castle is located at different positions. The broader peak observed in the wheelhouse is most probably caused by the way how the exhaust plume is dispersed around the ship

4. Discussion

Decision-makers who are responsible for improving living and working conditions need to receive objective, reliable, and understandable information about indoor air quality. It is only with such information that they gain understanding in the urgency of a problem and in the selection of the most appropriate mitigation action. One way to collect such information is to perform time-averaged measurements about the concentrations of pollutants with, for example, diffusion tubes and to compare the results with thresholds. Such analyses give a good insight in the safety of living and working conditions because they can be easily compared with occupational and nonoccupational thresholds (i.e., both must be considered because a ship is a working and a living place at the same time) as prescribed by legislation or recommended by highly regarded institutes. Such analyses make statements about the safety of the air the crew breathe and if actions are needed. Another way to evaluate the ship's indoor air quality is to compare the measurements with a benchmark that is associated to a certain public opinion: the quality of outdoor air in a large city. Brussels has been selected as that city because it is the largest city in Belgium and because the national monitoring stations in that city cover the broadest range of measured parameters that are publicly available. The time-averaged analyses performed on the ship indicate that most pollutant concentrations are below the mentioned thresholds. However, for several pollutants, the indoor air quality on board ship is comparable with the outdoor air in Brussels. Time-averaged analyses

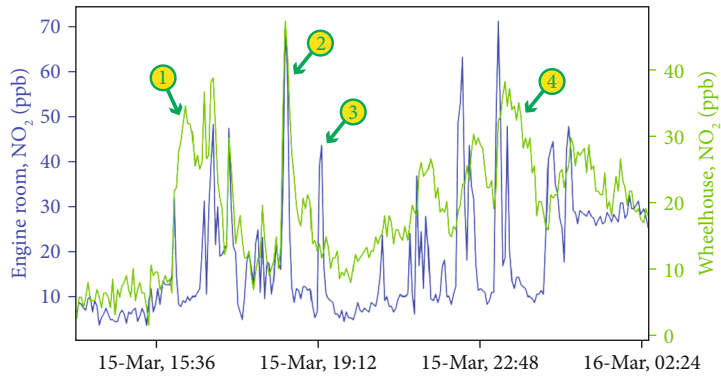

FIGURE 8: NO_2 trends measured with 2 sensor boxes in the wheelhouse and the engine room at exactly the same period while sailing. The trend of the engine room is a detail of the rectangle in Figure 7. Both locations are actively ventilated.

appear to give less information about the type of actions that are needed to improve the air quality.

This contribution shows that indoor air can be assessed with continuous-time measurements obtained with, for example, lower-cost sensor systems. The observed dynamics in the concentration trends of pollutants is an important source of information on the occurrence of (small) moments of worse air quality. This contribution has shown that there is a relationship between the occurrence of such peaks and the activity of pollution sources. The peaks can also be used to identify such sources. However, it is unclear how short moments of worse air quality affect human health. During one measurement campaign, the total exposure time to NO/NO_2 events is about 11% of the sailing period. Therefore, it would be better for the crew's health to avoid their occurrence. The ALARA principle states that better indoor air quality is achieved if the targeted actions to reduce the occurrence of pollution peaks are not too resource intensive, even when air quality is considered as sufficiently safe according to legislation.

This contribution has demonstrated that exhaust gas emitted by the funnel enters the ship's castle through the ventilation inlet. The strong fluctuations in the trends can be explained by the following phenomena: (1) the activity pattern of the engines affects the variation of emitted pollutant concentrations over time and thus the concentration at the ventilation inlet [81]; (2) the smaller the distance between funnel and inlet, the less diluted the exhaust gas is; (3) the wind direction relative to the motion of the ship; and (4) wind speed relative to the speed of the ship. This research suggests that indoor air quality can be improved by changing the position of the ventilation inlet.

5. Conclusions

The time-averaged TVOC analysis demonstrated that multiple organic compounds are present at low concentrations. However, the total amount of these compounds is significantly higher than its individual products. The TVOC is underestimated when organic compounds remain invisible for the analytical method. When performing time-averaged analyses using Radiello tubes, the impact of high but narrow peaks on the crew's health remains unnoticed because they do not affect the average concentration significantly. In addition, the impact of high but narrow peaks with a width of 1 hour down to a few minutes is probably also underestimated by the methods prescribed by legislation where air quality is assessed by considering the average concentrations of the past 15 minutes or 8 hours. The measurements have also shown that the makeup of the mixture of organic compounds varies from location to location and with time.

The continuous-time measurement campaigns in a shipping context have shown that the temporal trend is inherently unstable for a large number of indoor environmental parameters. In addition, dynamics in the trends measured at the same location but at different moments or the trends measured at different locations at the same time are always different and therefore unique. It suggests that the distribution of pollutants across a ship is heterogeneous and changes over time. All pollutants show peaks at well-defined moments superposed on a slower fluctuating background. For ozone, also valleys on a higher background concentration have been observed.

When analysing the peaks in the trends, some of them occur at the same time. This suggests that they are caused by the same pollution source. Exhaust gases are responsible for a pattern of NO-NO_2-CO-TVOC peaks. They are also responsible for CO-TVOC peak correlations preceded by a PM peak. The peaks show that exhaust gases can enter all interior spaces of the ship via the ventilation system. Human presence is related to a CO_2-RH-T pattern. The situation for PM is more complex. In the wheelhouse, some PM peaks are probably caused by human presence due to swirling dust at the vicinity of the measuring instruments. In the engine room, pumps or generators that are regularly switched on can cause dust to be resuspended via vibrations. Another pollution source that has been identified is the bunkering process where fuel vapours are released. The dynamics in the trends suggest that it is meaningful to monitor several parameters simultaneously.

A comparison of the air quality with nonoccupational thresholds shows that all analysed locations are sufficiently

safe for the crew, except for the storage room where ventilation needs to be improved. At that location, the TVOC concentration exceeds the intervention value. For the engine room and the cabin, the TVOC guideline value has been exceeded. When compared with the outdoor air in Brussels, several indoor pollutants exceed the benchmark while others remain below. Yet, one can argue that the ship's indoor air is comparable with the outdoor air of a large city. The air quality can be improved when the infiltration of exhaust gases through the ventilation system is avoided.

Data Availability

All data used in this study are available upon request.

Additional Points

Practical Implications. This study reports a wide range of indoor air quality analyses. The time-averaged measurements of gaseous and particulate pollutants can easily be compared with thresholds to determine if work and living conditions are sufficiently safe. Monitoring campaigns give an insight in the fluctuations of the concentration of pollutants over time. The peaks and valleys in the temporal trends give additional information about the pollution source that affects the indoor air quality. Therefore, the trends give actionable information to decision-makers about how the indoor air quality can be improved.

Conflicts of Interest

The authors declare no conflict of interest.

Authors' Contributions

Borislav Lazarov and Marianne Stranger organized the installation of the reference monitoring systems on board ship. Borislav Lazarov has built the sensor shield of the sensor box and has calibrated the sensors. Gustavo Carro was responsible for the software development to visualize the collected data and to generate the images. The paper is written by Olivier Schalm and reviewed/edited by Werner Jacobs. Finally, Olivier Schalm is responsible for the conceptualization of the paper.

Acknowledgments

The authors thank Flanders Innovation & Entrepreneurship (VLAIO) for the financial support of the TETRA-project ELGAS (project number HBC.2019.2033), and the APC was funded with the cofinancing from the several participating organizations. The authors also thank Joeri Verbiest and Lorenz Adriaensen of Karel de Grote University of Applied Sciences and Arts and the following organizations for their contribution in the project: Engine Deck Repair (EDR), Mediport, eu.reca, Kenniscentrum Binnenvaart Vlaanderen, De Vlaamse Waterweg, Jan De Nul, General Bunkering Services (GBS), AllThingsTalk, LCL, Telenet Group BVBA, and Atmosafe.

Supplementary Materials

(i) Graphical abstract of the article showing how exhaust gas causes pollution peaks in the ship's castle. See supplemental files. (ii) Supporting information about additional VOC analysis is available as an additional document. See supplemental files. *(Supplementary Materials)*

References

[1] Z. Liu, X. Lu, J. Feng, Q. Fan, Y. Zhang, and X. Yang, "Influence of ship emissions on urban air quality: a comprehensive study using highly time-resolved online measurements and numerical simulation in Shanghai," *Environmental Science & Technology*, vol. 51, no. 1, pp. 202–211, 2017.

[2] D. Mueller, S. Uibel, M. Takemura, D. Klingelhoefer, and D. A. Groneberg, "Ships, ports and particulate air pollution - an analysis of recent studies," *Journal of Occupational Medicine and Toxicology*, vol. 6, no. 1, p. 31, 2011.

[3] X. Wang, Y. Shen, Y. Lin et al., "Atmospheric pollution from ships and its impact on local air quality at a port site in Shanghai," *Atmospheric Chemistry and Physics*, vol. 19, no. 9, pp. 6315–6330, 2019.

[4] Y. Zhang, X. Yang, R. Brown et al., "Shipping emissions and their impacts on air quality in China," *Science of The Total Environment*, vol. 581-582, pp. 186–198, 2017.

[5] L. Bencs, B. Horemans, A. J. Buczyńska, and R. Van Grieken, "Uneven distribution of inorganic pollutants in marine air originating from ocean-going ships," *Environmental Pollution*, vol. 222, pp. 226–233, 2017.

[6] V. Eyring, "Emissions from international shipping: 2. Impact of future technologies on scenarios until 2050," *Journal of Geophysical Research*, vol. 110, no. D17, p. 18, 2005.

[7] S. Langer, C. Österman, B. Strandberg, J. Moldanová, and H. Fridén, "Impacts of fuel quality on indoor environment onboard a ship: from policy to practice," *Transportation Research Part D: Transport and Environment*, vol. 83, article 102352, 2020.

[8] K. Lehtoranta, P. Aakko-Saksa, T. Murtonen et al., "Particulate mass and nonvolatile particle number emissions from marine engines using low-sulfur fuels, natural gas, or scrubbers," *Environmental Science & Technology*, vol. 53, no. 6, pp. 3315–3322, 2019.

[9] W. Peng, J. Yang, J. Corbin et al., "Comprehensive analysis of the air quality impacts of switching a marine vessel from diesel fuel to natural gas," *Environmental Pollution*, vol. 266, Part 3, article 115404, 2020.

[10] J. Zhao, Q. Wei, S. Wang, and X. Ren, "Progress of ship exhaust gas control technology," *Science of The Total Environment*, vol. 799, article 149437, 2021.

[11] L. Tao, D. Fairley, M. J. Kleeman, and R. A. Harley, "Effects of switching to lower sulfur marine fuel oil on air quality in the San Francisco Bay Area," *Environmental Science & Technology*, vol. 47, no. 18, pp. 10171–10178, 2013.

[12] X. Zhang, Y. Zhang, Y. Liu et al., "Changes in the SO2 level and PM2.5 components in Shanghai driven by implementing the ship emission control policy," *Environmental Science & Technology*, vol. 53, no. 19, pp. 11580–11587, 2019.

[13] J. J. Corbett, J. J. Winebrake, E. H. Green, P. Kasibhatla, V. Eyring, and A. Lauer, "Mortality from ship emissions: a

global assessment," *Environmental Science & Technology*, vol. 41, no. 24, pp. 8512–8518, 2007.

[14] S. S. Kim and Y. G. Lee, "Field measurements of indoor air pollutant concentrations on two new ships," *Building and Environment*, vol. 45, no. 10, pp. 2141–2147, 2010.

[15] J. J. Corbett, "Updated emissions from ocean shipping," *Journal of Geophysical Research*, vol. 108, no. D20, p. 4650, 2003.

[16] P. De Meyer, F. Maes, and A. Volckaert, "Emissions from international shipping in the Belgian part of the North Sea and the Belgian seaports," *Atmospheric Environment*, vol. 42, no. 1, pp. 196–206, 2008.

[17] V. Eyring, "Emissions from international shipping: 1. The last 50 years," *Journal of Geophysical Research*, vol. 110, no. D17, p. D17305, 2005.

[18] IMO, *Third IMO greenhouse gas study 2014: executive summary and final report*, International Maritime Organization, 2015.

[19] L. Schrooten, I. De Vlieger, L. Int Panis, K. Styns, and R. Torfs, "Inventory and forecasting of maritime emissions in the Belgian sea territory, an activity-based emission model," *Atmospheric Environment*, vol. 42, no. 4, pp. 667–676, 2008.

[20] A. J. Baird and R. N. Pedersen, "Analysis of CO_2 emissions for island ferry services," *Journal of Transport Geography*, vol. 32, pp. 77–85, 2013.

[21] H. Agrawal, W. A. Welch, S. Henningsen, J. W. Miller, and D. R. Cocker, "Emissions from main propulsion engine on container ship at sea," *Journal of Geophysical Research*, vol. 115, no. D23, p. 7, 2010.

[22] C. Huang, Q. Hu, H. Wang et al., "Emission factors of particulate and gaseous compounds from a large cargo vessel operated under real-world conditions," *Environmental Pollution*, vol. 242, Part A, pp. 667–674, 2018.

[23] D. Chen, Y. Zhao, P. Nelson et al., "Estimating ship emissions based on AIS data for port of Tianjin, China," *Atmospheric Environment*, vol. 145, pp. 10–18, 2016.

[24] L. Huang, Y. Wen, Y. Zhang, C. Zhou, F. Zhang, and T. Yang, "Dynamic calculation of ship exhaust emissions based on real-time AIS data," *Transportation Research Part D: Transport and Environment*, vol. 80, article 102277, 2020.

[25] D. Busch and K. Krause, "Air quality on the Rhine and in the inland ports of Duisburg and Neuss –," *Immissionsschutz.*, vol. 26, no. 2, p. 9, 2021.

[26] F. Ledoux, C. Roche, F. Cazier, C. Beaugard, and D. Courcot, "Influence of ship emissions on NO_x, SO_2, O_3 and PM concentrations in a North-Sea harbor in France," *Journal of Environmental Sciences*, vol. 71, pp. 56–66, 2018.

[27] J. Passig, J. Schade, R. Irsig et al., "Detection of ship plumes from residual fuel operation in emission control areas using single-particle mass spectrometry," *Atmospheric Measurement Techniques*, vol. 14, no. 6, pp. 4171–4185, 2021.

[28] L. Bencs, B. Horemans, A. J. Buczyńska et al., "Seasonality of ship emission related atmospheric pollution over coastal and open waters of the North Sea," *Atmospheric Environment*, vol. 7, article 100077, 2020.

[29] C. Wang, L. Hao, D. Ma et al., "Analysis of ship emission characteristics under real-world conditions in China," *Ocean Engineering*, vol. 194, article 106615, 2019.

[30] A. Bogdanowicz and T. Kniaziewicz, "Marine diesel engine exhaust emissions measured in ship's dynamic operating conditions," *Sensors*, vol. 20, no. 22, p. 6589, 2020.

[31] O. Schalm, G. Carro, B. Lazarov, W. Jacobs, and M. Stranger, "Reliability of lower-cost sensors in the analysis of indoor air quality on board ships," *Atmosphere*, vol. 13, no. 10, p. 1579, 2022.

[32] M. Y. Khan, S. Ranganathan, H. Agrawal et al., "Measuring in-use ship emissions with international and U.S. federal methods," *Journal of the Air & Waste Management Association*, vol. 63, no. 3, pp. 284–291, 2013.

[33] A. P. Ault, C. J. Gaston, Y. Wang, G. Dominguez, M. H. Thiemens, and K. A. Prather, "Characterization of the single particle mixing state of individual ship plume events measured at the port of Los Angeles," *Environmental Science & Technology*, vol. 44, no. 6, pp. 1954–1961, 2010.

[34] D. Pillot, B. Guiot, P. L. Cottier, P. Perret, and P. Tassel, "Exhaust emissions from in-service inland waterways vessels," *Journal of Earth Sciences and Geotechnical Engineering*, vol. 6, no. 4, pp. 205–225, 2016.

[35] D. A. Cooper, "Exhaust emissions from high speed passenger ferries," *Atmospheric Environment*, vol. 35, no. 24, pp. 4189–4200, 2001.

[36] D. Cooper, "Exhaust emissions from ships at berth," *Atmospheric Environment*, vol. 37, no. 27, pp. 3817–3830, 2003.

[37] D. Cooper and M. Ekstrom, "Applicability of the PEMS technique for simplified NO monitoring on board ships," *Atmospheric Environment*, vol. 39, no. 1, pp. 127–137, 2005.

[38] D. A. Cooper and K. Andreasson, "Predictive NO_x emission monitoring on board a passenger ferry," *Atmospheric Environment*, vol. 33, no. 28, pp. 4637–4650, 1999.

[39] A. Anand, P. Wei, N. K. Gali et al., "Protocol development for real-time ship fuel sulfur content determination using drone based plume sniffing microsensor system," *Science of The Total Environment*, vol. 744, article 140885, 2020.

[40] X. Peng, L. Huang, L. Wu et al., "Remote detection sulfur content in fuel oil used by ships in emission control areas: a case study of the Yantian model in Shenzhen," *Ocean Engineering*, vol. 237, article 109652, 2021.

[41] P. Sinha, P. V. Hobbs, R. J. Yokelson, T. J. Christian, T. W. Kirchstetter, and R. Bruintjes, "Emissions of trace gases and particles from two ships in the southern Atlantic Ocean," *Atmospheric Environment*, vol. 37, no. 15, pp. 2139–2148, 2003.

[42] W. Van Roy, K. Scheldeman, B. Van Roozendael et al., "Airborne monitoring of compliance to NO_x emission regulations from ocean-going vessels in the Belgian North Sea," *Atmospheric Pollution Research*, vol. 13, no. 9, article 101518, 2022.

[43] C. Yu, D. Pasternak, J. Lee et al., "Characterizing the particle composition and cloud condensation nuclei from shipping emission in Western Europe," *Environmental Science & Technology*, vol. 54, no. 24, pp. 15604–15612, 2020.

[44] W. Van Roy, R. Schallier, B. Van Roozendael, K. Scheldeman, A. Van Nieuwenhove, and F. Maes, "Airborne monitoring of compliance to sulfur emission regulations by ocean- going vessels in the Belgian North Sea area," *Atmospheric Pollution Research*, vol. 13, no. 6, article 101445, 2022.

[45] D. Chen, X. Fu, X. Guo et al., "The impact of ship emissions on nitrogen and sulfur deposition in China," *Science of The Total Environment*, vol. 708, article 134636, 2020.

[46] A. Ekmekçioğlu, S. L. Kuzu, K. Ünlügençoğlu, and U. B. Çelebi, "Assessment of shipping emission factors through monitoring and modelling studies," *Science of The Total Environment*, vol. 743, article 140742, 2020.

[47] E. Chianese, G. Tirimberio, L. Appolloni et al., "Chemical characterisation of PM10 from ship emissions: a study on samples from hydrofoil exhaust stacks," *Environmental Science and Pollution Research*, vol. 29, no. 12, pp. 17723–17736, 2022.

[48] Q. Xiao, M. Li, H. Liu et al., "Characteristics of marine shipping emissions at berth: profiles for particulate matter and volatile organic compounds," *Atmospheric Chemistry and Physics*, vol. 18, no. 13, pp. 9527–9545, 2018.

[49] H. Agrawal, Q. G. J. Malloy, W. A. Welch, J. Wayne Miller, and D. R. Cocker, "In-use gaseous and particulate matter emissions from a modern ocean going container vessel," *Atmospheric Environment*, vol. 42, no. 21, pp. 5504–5510, 2008.

[50] H. Agrawal, W. A. Welch, J. W. Miller, and D. R. Cocker, "Emission measurements from a crude oil tanker at sea," *Environmental Science & Technology*, vol. 42, no. 19, pp. 7098–7103, 2008.

[51] P. Eichler, M. Müller, C. Rohmann et al., "Lubricating oil as a major constituent of ship exhaust particles," *Environmental Science & Technology Letters*, vol. 4, no. 2, pp. 54–58, 2017.

[52] W. Jacobs, *Cargo Vapour Concentrations on Board Chemical Tankers in the Non-Cargo Area during Normal Operations, [Ph.D. thesis]*, Antwerp Maritime Academy, 2019.

[53] W. Jacobs, C. Reynaerts, S. Andries, S. van den Akker, N. Moonen, and D. Lamoen, "Analyzing the dispersion of cargo vapors around a ship's superstructure by means of wind tunnel experiments," *Journal of Marine Science and Technology*, vol. 21, no. 4, pp. 758–766, 2016.

[54] W. Jacobs, D. Dubois, D. Aerts et al., "Monitoring of some major volatile organic compounds on board of chemical tankers," *Journal of Maritime Research*, vol. 7, no. 2, pp. 3–20, 2010.

[55] S. Langer, J. Moldanová, E. Bloom, and C. Österman, "Indoor environment on-board the Swedish icebreaker Oden," *Proceedings of Indoor Air 2014*, , International Society for Indoor Air Quality and Climate (ISIAQ), p. 8, 2014.

[56] M. Panaitescu, F. V. Panaitescu, M. V. Dumitrescu, and V. N. Panaitescu, "The impact of quality air in the engine room on the crew," *The International Journal on Marine Navigation and Safety of Sea Transportation*, vol. 13, no. 2, pp. 409–414, 2019.

[57] D. K. Farmer, M. E. Vance, J. P. D. Abbatt et al., "Overview of HOMEChem: house observations of microbial and environmental chemistry," *Environmental Science: Processes & Impacts*, vol. 21, no. 8, pp. 1280–1300, 2019.

[58] K. K. Lee, R. Bing, J. Kiang et al., "Adverse health effects associated with household air pollution: a systematic review, meta-analysis, and burden estimation study," *The Lancet Global HealthHealth*, vol. 8, no. 11, pp. e1427–e1434, 2020.

[59] J. Saini, M. Dutta, and G. Marques, "A comprehensive review on indoor air quality monitoring systems for enhanced public health," *Sustainable Environment Research*, vol. 30, no. 1, p. 6, 2020.

[60] S. Vardoulakis, E. Giagloglou, S. Steinle et al., "Indoor exposure to selected air pollutants in the home environment: a systematic review," *International Journal of Environmental Research and Public Health*, vol. 17, no. 23, p. 8972, 2020.

[61] W. Anaf and O. Schalm, "Climatic quality evaluation by peak analysis and segregation of low-, mid-, and high-frequency fluctuations, applied on a historic chapel," *Building and Environment*, vol. 148, pp. 286–293, 2019.

[62] G. Carro, O. Schalm, W. Jacobs, and S. Demeyer, "Exploring actionable visualizations for environmental data: air quality assessment of two Belgian locations," *Environmental Modelling and Software*, vol. 147, article 105230, 2022.

[63] B. Lazarov, R. Swinnen, M. Spruyt et al., "Optimisation steps of an innovative air sampling method for semi volatile organic compounds," *Atmospheric Environment*, vol. 79, pp. 780–786, 2013.

[64] J. Alanen, M. Isotalo, N. Kuittinen et al., "Physical characteristics of particle emissions from a medium speed ship engine fueled with natural gas and low-sulfur liquid fuels," *Environmental Science & Technology*, vol. 54, no. 9, pp. 5376–5384, 2020.

[65] T. Chu-Van, Z. Ristovski, A. M. Pourkhesalian et al., "On-board measurements of particle and gaseous emissions from a large cargo vessel at different operating conditions," *Environmental Pollution*, vol. 237, pp. 832–841, 2018.

[66] N. Kuittinen, J. P. Jalkanen, J. Alanen et al., "Shipping remains a globally significant source of anthropogenic PN emissions even after 2020 sulfur regulation," *Environmental Science & Technology*, vol. 55, no. 1, pp. 129–138, 2021.

[67] W. Anaf, D. Leyva Pernia, and O. Schalm, "Standardized indoor air quality assessments as a tool to prepare heritage guardians for changing preservation conditions due to climate change," *Geosciences Journal*, vol. 8, no. 8, p. 276, 2018.

[68] O. Schalm, A. Cabal, W. Anaf, D. Leyva Pernia, J. Callier, and N. Ortega, "A decision support system for preventive conservation: from measurements towards decision making," *The European Physical Journal Plus*, vol. 134, no. 2, p. 74, 2019.

[69] Belgium, "Codex on well-being at work (book VI, Title 1)," 2019, https://werk.belgie.be/nl/themas/welzijn-op-het-werk/algemene-beginselen/codex-over-het-welzijn-op-het-werk.

[70] EU, *Directive 2004/37/EC on exposure to carcinogens or mutagens at work*, European Union, 2004.

[71] EU, *Directive 98/24/EC on the protection of the health and safety of workers from the risks related to chemical agents at work*, European Union, 1998.

[72] Flanders, "Binnenmilieubesluit. Vol 2018013405," 2018, https://www.ejustice.just.fgov.be/cgi/welcome.pl.

[73] Belgian Interregional Environment Agency, "(IRCEL - CELINE) — English," May2022, https://www.irceline.be/en/front-page?set_language=en.

[74] K. Ravindra, A. C. Dirtu, S. Mor, E. Wauters, and R. Van Grieken, "Source apportionment and seasonal variation in particulate PAHs levels at a coastal site in Belgium," *Environmental Science and Pollution Research*, vol. 27, no. 13, pp. 14933–14943, 2020.

[75] International Maritime Organization (IMO), *Revised minimum safety standards for ships carrying liquids in bulk containing benzene (MSC/Circ. 1095)*, 2003.

[76] C. Jia and S. Batterman, "A critical review of naphthalene sources and exposures relevant to indoor and outdoor air," *International Journal of Environmental Research and Public Health*, vol. 7, no. 7, pp. 2903–2939, 2010.

[77] K. Ravindra, R. Sokhi, and R. Vangrieken, "Atmospheric polycyclic aromatic hydrocarbons: source attribution, emission factors and regulation," *Atmospheric Environment*, vol. 42, no. 13, pp. 2895–2921, 2008.

[78] K. Ravindra, L. Bencs, E. Wauters et al., "Seasonal and site-specific variation in vapour and aerosol phase PAHs over Flanders (Belgium) and their relation with anthropogenic

activities," *Atmospheric Environment*, vol. 40, no. 4, pp. 771–785, 2006.

[79] P. A. Leighton, *Photochemistry of Air Pollution*, Academic press, 1961.

[80] L. Clapp, "Analysis of the relationship between ambient levels of O_3, NO_2 and NO as a function of NO_x in the UK," *Atmospheric Environment*, vol. 35, no. 36, pp. 6391–6405, 2001.

[81] C. McCaffery, H. Zhu, G. Karavalakis, T. D. Durbin, J. W. Miller, and K. C. Johnson, "Sources of air pollutants from a tier 2 ocean-going container vessel: main engine, auxiliary engine, and auxiliary boiler," *Atmospheric Environment*, vol. 245, article 118023, 2021.